molbank

MDPI

Communication

# Synthesis and Spectroscopic Studies of Novel Dichloro and Polymethoxy p-Nitrophenyl Hydrazones:A Comparative Study.

**Sodeeq Babalola.[1]*, Nosakhare Igie[2], Abullah Idris.[1], Sanni Yeken.[1], Asmau Hamza[1], Hayatudeen Muhammad[1], Oshoma Erumiseli and Lateef Bakare[1]**

[1] Ahmadu Bello University, Zaria; ndagiginda59@gmail.com
[2] b Department of Chemistry and Biochemistry, The University of Texas at Dallas, Richardson,, USA.; nosakhare.igie@utdallas.edu
* Correspondence: wale.babalola91@gmail.com; Tel.: +2347058199796 ORCID: 0000-0003-0580-0595

**Abstract:** We conducted a comparative study on the development of two synthetic methods. The solvent-free synthesis is a green chemistry method developed in a bid to ameliorate environmental adverse effects of the conventional solvent-based synthesis. The synthesis of novel dichloro and polymethoxy p-nitrophenylhydrazones through solvent free technique gave moderate to high yields which were however lower than those of the solvent-based method. The established solvent-free approach has several benefits, including universality and simplicity of the approach, catalyst-free conditions, non-use of an organic solvent, quick reaction time, fast and efficient workup, and un-solvated pure products in moderate to high yields.

**Keywords**: p-nitrophenyl hydrazone; solvent-free; green synthesis; p-nitrophenyl hydrazine; mechanochemistry; dichloro p-nitrophenyl hydrazone; methoxy p-nitrophenyl hydrazone; solvent-based; spectroscopy; elucidation

**Citation:** Babalola, S.; Igie, N.; Idris, A., Sanni Y., Hamza A., Hayatudeen M., Oshoma E., Lateef B. synthesis, and spectroscopic studies of novel dichloro and polymethoxy p-nitrophenyl hydrazones; a comparative study. *Molbank* **2022**, *2022*, x. https://doi.org/10.3390/xxxxx

Academic Editor: First name Last-name

Received: date
Accepted: date
Published: date



## 1. Introduction

The importance of new chemical entities is to leverage the drawbacks in drug discovery research. This gives synthetic chemists the impetus to discover novel molecules with improved properties or novel methodologies to access these molecules with high efficiency. Organic synthesis can result in major or minor modifications to form new compounds, or modifications to the existing synthetic methodology to form new molecules with improved yield. Low yield, high energy requirements, and longer reaction time are the limitations of conventional synthetic methodologies involving heating reactants by certain heat energy sources [1].

For a long time, several research techniques have been innovated for the development of environmentally benign reactions, which are both cost-effective and technologically feasible [2-3]. The green chemistry campaign started under the pollution prevention legislation way back in 1990 [2], this legislation has given rise to the development of new technologies and techniques such as ultrasound, microwave, photochemical, and/or mechanical devices needed to perform environmentally friendly reactions. Furthermore, this legislation has publicized the production of organic compounds in greener ways [2-6]. Environmentally friendly synthetic processes have gotten a lot of attention recently, and certain solvent-free protocols have been established [7]. Because of the method's selectivity, it has resulted in fewer by-products and their elimination during purification stages seen in pharmaceutical ingredients and treatments.

The mechanochemistry technique has gained an upsurge of popularity, given its shorter reaction time, efficient reactions with minimal energy requirement, good to excellent yield, simpler work-up procedures advantages, with the use of solvent-free or solid-

state synthesis over conventional solvent-based synthesis [7]. Conventional solvent-based methods employ volatile organic compounds (VOC) and other toxic chemicals leading to releases of hazardous effluents and their resultant environmental problems [2,4,5] and genetic mutations on human health with consequent disorders including cancers.

Chlorobenzaldehydes have found usefulness in the pharmaceutical industry, especially in the synthesis of active pharmaceutical ingredients (API). The formation of the C-N bond is of importance as it allows the incorporation of nitrogen into organic compounds such as heterocycles. However, the formation of this bond remains a major challenge to organic chemists due to unfavorable reaction conditions and the cost of catalysts [8].

Hydrazones have a wide spectrum of applicability in synthetic chemistry as synthetic intermediates in the formation of medicinally important heterocyclic compounds, also as ligands in complex formation. Compounds with hydrazone functional group have found essential roles in organic synthesis due to their nucleophilic and electrophilic characters as an intermediate in Mannich type reactions, Wolf-Kishner reaction, asymmetric hydrocyanation, Mitsunobu reactions, and allylation [9]. Until recently, hydrazones were mostly synthesized employing traditional procedures, which involved reacting hydrazine with carbonyl molecule in diluted media under reflux conditions. Mo *et al*. reported the synthesis of a series of hydrazones in a 1:1 aqueous ethanol media catalyzed by meglumine. The condensation of phenylhydrazine with benzaldehydes substituted with an electron-withdrawing or electron-donating groups produced high to excellent yields of the titled hydrazones [10]. By refluxing an equimolar amount of 2-Amino-3-formyl chromone and hydrazide derivatives in acetic acid, Noor *et al*. reported the synthesis of new hydrazones. The reaction gave high to excellent yields of the hydrazone products [11]. In methanol, Jana *et al*. synthesized hydrazones by condensation of dihydroxybenzaldehyde with hydrazide derivatives. The reactions' products were obtained in high yields [12].

Also, a handful of solvent-free syntheses of hydrazones have been described in the literature. Pierrick *et al*. reported the solvent-free synthesis of Boc-, Bz-, Fmoc-, and tosyl-hydrazones from aldehydes in a ball mill [13]. The development of the solvent-free synthesis of hydrazones catalyzed by Bronsted acid ionic liquid (BAIL) [Et3NH][HSO4] was reported by Mehtab *et al*. [14]. Oliveira *et al*. also reports a solvent-free mechanochemistry synthesis of a series of therapeutically active phenol hydrazones [15]. Microwave-assisted synthesis of oxobenzotriazine hydrazides under solvent-free conditions has also been studied by Harith and Aymen [16]. The microwave-assisted synthesis of corrosion inhibitors series of thiophene hydrazones under solvent-free solvent-free conditions were described by Singh *et al*. [17]. Crawford *et al*. used Twin-Screw Extrusion to synthesize hydrazone-base active medicinal components in a solvent-free and continuous flow process [18]. Hydrazone derivatives have a wide range of biological properties and are commonly used as medicines. The possible applications of hydrazones as anti-diuretic, antioxidants, anti-inflammatory, anti-sepsis, anti-parkinsonism, anti-tuberculosis agents, analgesic, anti-ulcer, vasodilators for hypertension treatment, anti-ageing, central nervous system diseases, anticancer agents, anti-neoplastic, antimicrobial, anti-depressant, anti-convulsant, antiviral, anti-arrhythmic, antimycobacterial, antimalarial, antiplatelet, anti-histaminic demonstrate that the hydrazone class is essential for new drug development [19-34]. The discovery of hydrazone drugs such as levosimendan, dantrolene, nitrofurantoin, nitrofurazone, furazolidone, and nifuroxazide indicate that hydrazone moiety is a privileged scaffold. Here, we report the total synthesis, and spectroscopic studies of novel dichloro and polymethoxy p-nitrophenyl hydrazones, highlighting its comparative studies on solvent-based and solvent-free methods.

## 2. Results

*2.1. Condensation reaction methods*

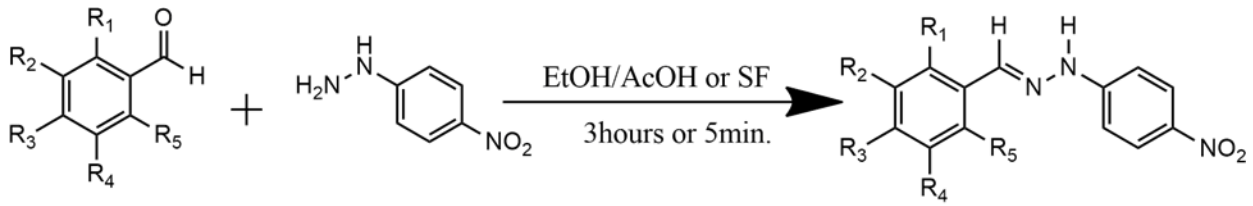


1 2 3

**Scheme 1.** Synthesis of p-nitrophenyl hydrazones.

| Compound | $R_1$ | $R_2$ | $R_3$ | $R_4$ | $R_5$ |
|---|---|---|---|---|---|
| **3a** | Cl | H | Cl | H | H |
| **3b** | H | Cl | H | Cl | H |
| **3c** | H | $OCH_3$ | $OCH_3$ | $OCH_3$ | H |
| **3d** | H | H | $OCH_3$ | H | H |

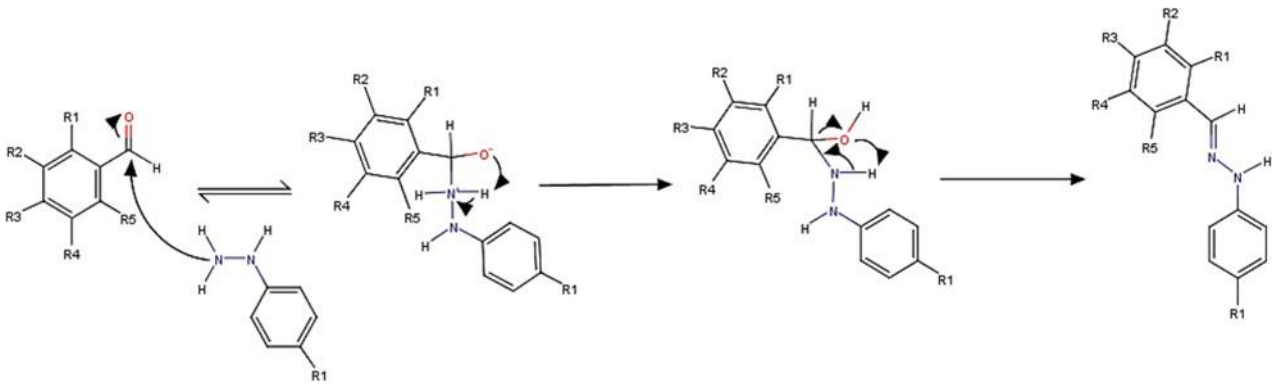

**Scheme 2.** Solvent-free mechanism of the reaction.

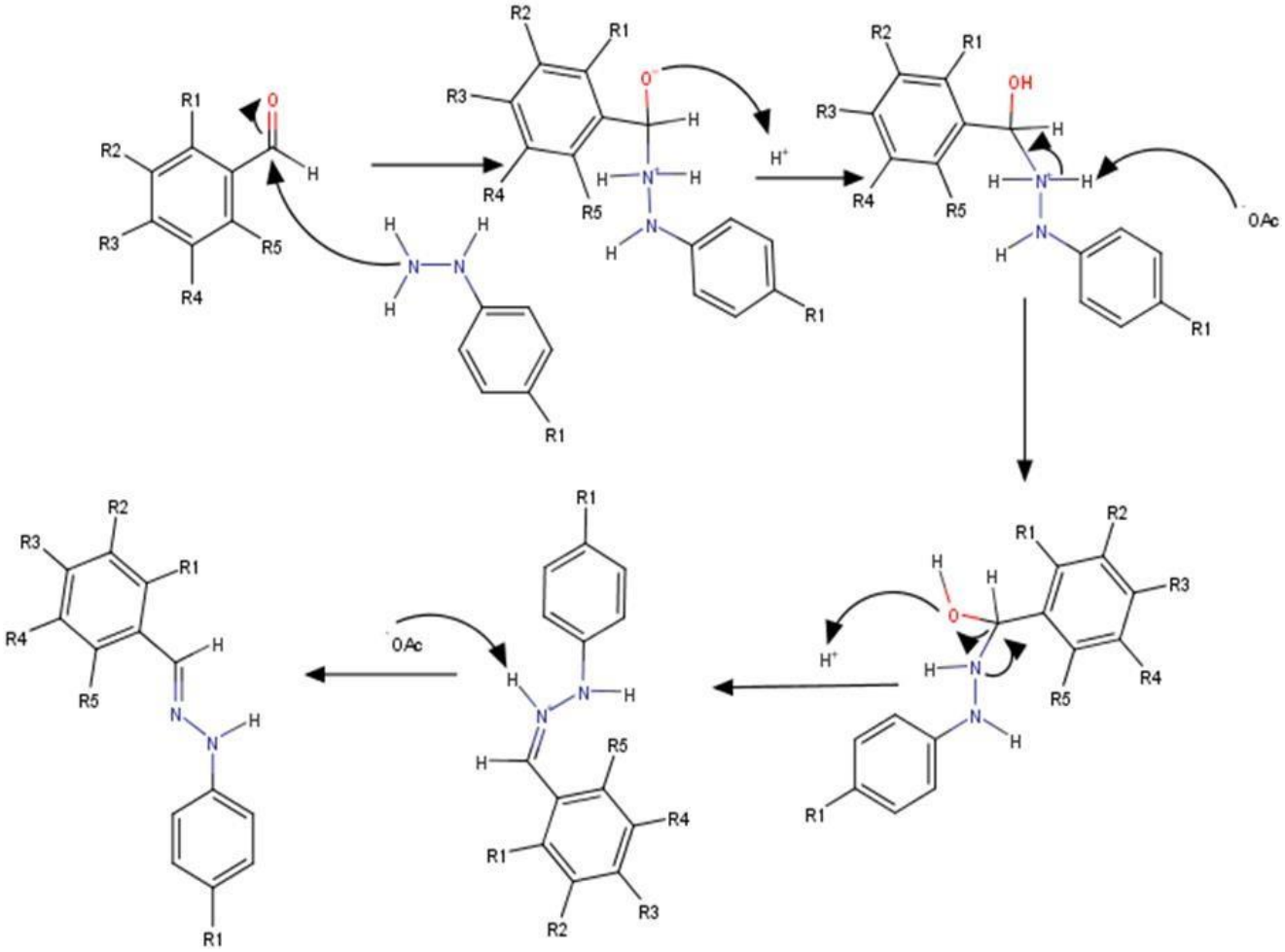

**Scheme 3.** Solvent-based reaction mechanism.

**Table 1**: Solvent-based and solvent-free synthesis of compounds **3a-d** results comparison under room conditions.

| | Solvent-free | | | Solvent-based | | |
|---|---|---|---|---|---|---|
| Compd | Time (min) | Yield (%) | Mp (ºC) | Time (h) | Yield (%) | Mp (ºC) |
| **3a** | 5 | 57.28 | 226-228 | 3 | 67.90% | 226-228 |
| **3b** | 5 | 32.69 | 257-259 | 3 | 72.36% | 257-259 |
| **3c** | 5 | 30.51 | 185-188 | 3 | 70.27% | 185-188 |
| **3d** | --- | --- | --- | 3 | 53.49% | 152-155 |

*2.2. Spectroscopy analysis results*

**Table 2**: FTIR data of the synthesized hydrazones ($cm^{-1}$).

| Compound | N-H | C-H$_{imine}$ | C=N | $NO_2$ | C-N$_{aniline}$ | C-Cl | CH$_{methoxy}$ | C-O-C | C=C$_{arom}$ | C-H$_{arom}$ |
|---|---|---|---|---|---|---|---|---|---|---|
| **3a** | 3265 | 3078 | 1587 | 1498 | 1300 | 1043 | ---- | ---- | 1461 | 1271 |
| **3b** | 3254 | 3075 | 1580 | 1476 | 1297 | 957 | ---- | ---- | 1416 | 1271 |
| **3c** | 3283 | 2929 | 1591 | 1494 | 1125 | ---- | 2840 | 1289 | 1412 | 1379 |
| **3d** | 3261 | 3000 | 1595 | 1509 | 1168 | ---- | 2832 | 1241 | 1468 | 127 |

**Table 3**: 1D and 2D NMR data for **3a** (ppm).

| Position | $\delta_H$ (*J* in Hz) | $\delta_C$, type | COSY | HSQC | HMBC |
|---|---|---|---|---|---|
| 1 | --- | 131.39, C | --- | --- | 3,5,7 |
| 2 | --- | 134.36, C | --- | --- | 3 |
| 3 | 7.65, d (1.8) | 129.71, CH | 5 | 3 | 1,2,5 |
| 4 | --- | 133.16, C | --- | --- | 6 |
| 5 | 7.47, d (8.5) | 128.29, CH | 3,6 | 5 | 1,3 |
| 6 | 8.05, d (8.6) | 127.98, CH | 5 | 6 | 4,7 |
| 7 | 8.29, s | 136.58, CH | N-H | 7 | 1,6,N-H |
| N-H | 11.61, s | --- | 7 | --- | (2′,6′),7 |
| 1′ | --- | 139.43, C | --- | --- | (2′,6′),(3′,5′) |
| 2′ | 7.18, d (8.2) | 112.10, CH | (3′,5′) | (2′,6′) | N-H,1′,(2′,6′),(3′.5′) |
| 3′ | 8.13, d (9.0) | 126.54, CH | (2′,6′) | (3′,5′) | 1′, (2′,6′), (3′,5′), 4′ |
| 4′ | --- | 150.43, C | --- | --- | (3′,5′) |
| 5′ | 8.13, d (9.0) | 126.54, CH | (2′,6′) | (3′,5′) | 1′, (2′,6′), (3′,5′), 4′ |
| 6′ | 7.18, d (8.2) | 112.10, CH | (3′,5′) | (2′,6′) | N-H,1′,(2′,6′),(3′.5′) |

**Table 4**: 1D and 2D NMR data for **3b** (ppm).

| Position | $\delta_H$ (*J* in Hz) | $\delta_C$, type | COSY | HSQC | HMBC |
|---|---|---|---|---|---|
| 1 | --- | 135.00, C | --- | --- | (2,6) |
| 2 | 7.79, s | 124.96, CH | 4 | (2,6) | 1,(2,6),4,7 |
| 3 | --- | 139.44, C | --- | --- | --- |
| 4 | 7.59, s | 128.38 | (2,6) | 4 | (2,6) |
| 5 | --- | 139.44, C | --- | --- | --- |
| 6 | 7.79, s | 124.96, CH | 4 | (2,6) | 1,4,7 |
| 7 | 7.98, s | 138.80, CH | N-H | 7 | N-H, (2,6), 7 |
| N-H | 11.55, s | --- | 7 | --- | (2′,6′), 7 |
| 1′ | --- | 135.00, C | --- | --- | --- |
| 2′ | 7.25, d (8.1) | 112.23, CH | (3′,5′) | (2′,6′) | N-H, (2′,6′) |
| 3′ | 8.16, d (9.1) | 126.50 | (2′,6′) | (3′,5′) | (3′,5′), 4′ |
| 4′ | --- | 150.52 | --- | --- | (3′,5′), 4′ |
| 5′ | 8.16, d (9.1) | 126.50 | (2′,6′) | (3′,5′) | (3′,5′), 4′ |
| 6′ | 7.25, d (8.1) | 112.23, CH | (3′,5′) | (2′,6′) | N-H, (2′,6′) |

**Table 5**: 1D and 2D NMR data for **3c** (ppm).

| Position | $\delta_H$ (*J* in Hz) | $\delta_C$, type | COSY | HSQC | HMBC |
|---|---|---|---|---|---|
| 3,5-OMe | 3.85, s | 56.35, $CH_3$ | --- | 3,5-OMe | 3,5 |
| 4-OMe | 3.69, s | 60.54, $CH_3$ | --- | 4-OMe | 4 |
| 1 | --- | 130.65, C | --- | --- | (2,6), 7 |
| 2 | 7.05, s | 104.15, CH | 7 | (2,6) | 1, (2,6), (3,5), 4, 7 |
| 3 | --- | 150.60, C | --- | --- | (2,6) |
| 4 | --- | 139.02, C | --- | --- | (2,6) |
| 5 | --- | 150.60, C | --- | --- | (2,6) |
| 6 | 7.05, s | 104.15, CH | 7 | (2,6) | 1, (2,6), (3,5), 4, 7 |
| 7 | 7.97, s | 142.24, CH | N-H | 7 | N-H, 1, (2,6) |
| N-H | 11.30, s | --- | 7 | --- | 1′, (2′,6′), 7 |
| 1′ | --- | 150.98, C | --- | --- | (3′,5′) |
| 2′ | 7.19, d (7.2) | 111.69, CH | (3′,5′) | (2′,6′) | N-H, (2′,6′), 4′ |
| 3′ | 8.13, d (8.7) | 126.58, CH | (2′,6′) | (3′,5′) | 1′, (2′,6′), (3′,5′), 4′ |
| 4′ | --- | 138.69, C | --- | --- | (2′,6′), (3′,5′) |
| 5′ | 8.13, d (8.7) | 126.58, CH | (2′,6′) | (3′,5′) | 1′, (2′,6′), (3′,5′), 4′ |
| 6′ | 7.19, d (7.2) | 111.69, CH | (3′,5′) | (2′,6′) | N-H, (2′,6′), 4′ |

**Table 6**: 1D and 2D NMR data for **3d** (ppm).

| Position | $\delta_H$ (*J* in Hz) [35] | $\delta_C$, type[35] | COSY | HSQC | HMBC |
|---|---|---|---|---|---|
| 4-OMe | 3.79, s | 55.70, $CH_3$ | --- | 4-OMe | 4 |
| 1 | --- | 127.68, C | --- | --- | (3,5) |
| 2 | 7.66, d (8.2) | 128.48, CH | (3,5) | (2,6) | 1, (2,6), (3,5), 4, 7 |
| 3 | 6.99, d (8,2) | 114.74, CH | (2,6) | (3,5) | 1, (2,6), (3,5), 4 |
| 4 | --- | 160.70, C | --- | --- | (2,6), (3,5), OMe |
| 5 | 6.99, d (8,2) | 114.74, CH | (2,6) | (3,5) | 1, (2,6), (3,5), 4 |
| 6 | 7.66, d (8.2) | 128.48, CH | (3,5) | (2,6) | 1, (2,6), (3,5), 4, 7 |
| 7 | 7.99, s | 142.41, CH | N-H | 7 | N-H, 1, (2,6) |
| N-H | 11.18, s | --- | 7 | 7 | (2′, 6′), 7 |
| 1′ | --- | 138.39, C | --- | --- | (2′,6′), (3′,5′) |
| 2′ | 7.12, d (7.0) | 111.43, CH | (3′,5′) | (2′,6′) | N-H, 1′, (2′,6′) |
| 3′ | 8.11, d (8.8) | 126.65, CH | (2′,6′) | (3′,5′) | 1′, (2′,6′), (3′,5′), 4′ |
| 4′ | --- | 151.15, C | --- | --- | (3′,5′) |
| 5′ | 8.11, d (8.8) | 126.65, CH | (2′,6′) | (3′,5′) | 1′, (2′,6′), (3′,5′), 4′ |
| 6′ | 7.12, d (7.0) | 111.43, CH | (3′,5′) | (2′,6′) | N-H, 1′, (2′,6′) |

## 3. Discussion

We report the comparative study on the synthesis of p-nitrophenyl hydrazones involving solvent-free and solvent-based condensation of p-nitrophenyl hydrazine with benzaldehydes having an electron-donating group or electron-withdrawing group which was carried out at room temperature.

### *3.1. Solvent-free*

The solvent-free synthesis of three novel para-nitrophenyl hydrazones was cleanly and efficiently performed in short reaction times without using any acid catalyst under solventless conditions and at room temperature. 4-nitrophenyl hydrazine 1 was condensed with aromatic aldehydes having electron-withdrawing or electron-donating groups (2,4-dichloro benzaldehyde, 3,5-dichloro benzaldehyde, 3,4,5-trimethoxy benzaldehyde, and 4-methoxy benzaldehyde). The hydrazones 3a-d were prepared by the reaction between the equimolar quantity of 4-nitrophenyl hydrazine and the said aromatic aldehyde 2a-d in solvent-free condition during 2-5 minutes at room condition.

### *3.2. Solvent-based*

The solvent-based synthesis investigates the condensation of the equimolar quantity of p-nitrophenylhydrazine 1 with each of the benzaldehydes 2 (2,4-dichlorobenzaldehyde, 3,4-dichlorobenzaldehyde, 4-methoxybenzaldehyde, and 3,4,5-trimethoxybenzaldehyde) in 30 ml of ethanol catalyzed by five drops of glacial acetic acid at room conditions. The reaction was allowed for three hours. Surprisingly, the products were formed within the first hour of the reactions. It has long been known that electron-withdrawing groups can increase the reactivity of aldehydes in hydrazone formation. Reaction with 2,4-dichlorobenzaldehyde was the fastest due to the inductive effect and the resultant increased electrophilic strength of the carbonyl carbon. Reaction with 3,5-dichlorobenzaldehyde was slower although with a better yield than that of 2,4-dichlorobenzaldehyde due to the reduced electrophilic character of the carbonyl carbon. The presence of the MeO group on the aldehyde ring allows for effective reactions with almost any substituent combination. It was observed that the reactivity trend favored electron-deficient aldehyde over electron-rich counterparts. The slowest reacting compound in the study was with 3,4,5-trimethoxybenzaldehyde.

All the reactions with p-nitrophenyl hydrazine afforded powdered products with slight color variation. The solvent-based method gave better yields compared to the solvent-free method in this case. However, the solvent-free method had a faster reaction time with less energy requirement. Both methods required no need for an inert environment, had the same selectivity and purity. Each of the compounds was purified and isolated from the reaction mixture by washing with freshly prepared cold 2 M hydrochloric acid followed by cold distilled water and cold 95% ethanol step-wisely with high to excellent yields (67.90%-72.36%) for solvent-based method while moderate to high yields (30%-57%) for solvent-free. The results of these reactions are revealed in table 1 below.

Mechanistically, the rate-limiting step is the formation of tetrahedral addition carbinolamine. The first two steps are concerted which involved the formation of a carbon-nitrogen bond and the addition of a proton to the oxygen atom via acid-catalyzed hydrazine attack on the carbonyl carbon. Unlike the uncatalyzed solvent-free method, this step leads to the formation of zwitterion intermediate form of carbinolamine whose stability is pH and hydrazine basicity dependent. There could be intramolecular proton abstraction from the possibly formed zwitterion quaternary ammonium center in the solvent-free mechanism akin to acid protonation of the carbonyl oxygen in the solvent-based method. This aided the rapid intramolecular dehydration of the carbinolamine intermediate formed in the solvent-free method contrary to acid-catalyzed dehydration of the kinetically significant carbinolamine intermediate in the solvent-based method.

### *3.3. Spectroscopic studies.*

Tables 2, 3, 4, 5, and 6 revealed detailed elucidation of FTIR, 1D NMR: 1H-NMR, and 13C-NMR and 2D NMR: COSY, HSQC, and HMBC spectra of the synthesized dichloro and methoxy p-nitrophenyl hydrazones.

#### 3.3.1. Structure elucidation of compound 3a (chrome yellow powder).

**(*E*)-1-(2,4-dichlorobenzylidene)-2-(4-nitrophenyl)hydrazine**

For compound E-1-(2,4-dichloro benzylidene)-2-(4-nitrophenyl) hydrazine (3a), the disappearance of characteristic aldehyde signals on proton and carbon-13 NMR spectra and the emergence of a singlet peak at 8.29 ppm integrating for one proton on the proton NMR spectrum and a peak at 136.58 ppm on carbon-13 NMR spectrum in table 3 which was coupled to each other (8.31, 136.54) ppm on HSQC spectrum suggest the synthesis of a new bond. FTIR absorption signals at 3078 $cm^{-1}$ and 1587 $cm^{-1}$ in table 2 correspond to azomethine (imine) C-H bond and azomethine (imine) C=N bond stretchings confirming the formation of new azomethine bond.

The singlet peak at 11.61 ppm integrating for one hydrogen on proton NMR spectrum in table 3 was noticed to couple with no carbon on HSQC spectrum which illustrated the presence of secondary amino N-H bond as suggested by the observed FTIR absorption signal at 3254 $cm^{-1}$ in table 2 characteristics of secondary amino N-H bond. Additionally, this singlet peak signal at 11.61 ppm on the proton NMR spectrum in table 3 was coupled with a corresponding imine hydrogen singlet peak at 8.29 ppm on the COSY spectrum (11.63, 8.26) ppm indicates the formation of hydrazone functional group. Further, the correlation between a carbon-13 peak at 136.28 ppm with proton peak at 11.61 ppm on the HMBC spectrum (11.61, 136.28) ppm confirmed the formation of hydrazone functional group.

The upfield doublet peak at 7.18 ppm integrating for two hydrogens and the downfield doublet peak at 8.13 ppm integrating for two hydrogens on the proton NMR spectrum were coupled on COSY cross peak spectrum (8.14, 7.18) ppm which implies that four neighboring protons are on a di-substituted benzene ring. Their coupling constants 8.2 Hz and 9.0 Hz respectively suggest that each of the two hydrogens are ortho coupled. Furthermore, it was noticed that the upfield doublet proton peak at 7.18 ppm integrating for two hydrogens was found coupled with carbon-13 signal at 112.04 ppm on HSQC spectrum (7.18, 112.04) ppm which suggests that the two equivalent hydrogens are on two equivalent carbons. Also, the downfield doublet proton peak at 8.14 ppm integrating for two hydrogens was observed to couple to carbon-13 peak at 126.46 ppm on HSQC spectrum (8.14, 126.46) ppm indicate that these two equivalent hydrogens are also directly attached to the two equivalent carbons.

The carbon-13 signal at 150.43 ppm was found to correlate with the proton signal at 8.14 ppm (8.14, 150.43) ppm, and another carbon-13 signal at 139.43 ppm was also found to correlate with proton signals at 7.18 ppm (7.18, 139.43) ppm and 8.14 ppm (8.14, 139.43) ppm on HMBC spectrum. Furthermore, the peaks at 150.43 ppm and 139.43 ppm on the carbon-13 spectrum were observed to couple with no hydrogens on the HSQC spectrum which suggests that they are substituted aromatic carbons. Additionally, there is a correlation between the proton signal at 7.18 ppm and carbon-13 signal at 126.21 ppm (7.18, 126.21), and another correlation between the amino hydrogen at 11.61 ppm and carbon-signal at 111.81 ppm (11.61, 111.81) ppm on the HMBC spectrum. Also, the FTIR absorption signal at 1300 cm-1 corresponded to C-N bond stretching as indicated in table 2. All taken together and on careful analysis of these correlated HMBC signals together with HSQC and COSY correlations conform with ring B (hydrazine ring) of the synthesized compound and are numbered accordingly. The upfield signals (7.18, 112.04) suggests that the two aromatic C-H are at position 2′ and 6′ and are neighbor to another aromatic carbon that is directly attached with an electron-donating group, this was confirmed by (11.61, 111.81) ppm i.e N-H and C-2′, 6′ correlation indicates that the amino group is directly attached to the carbon with 139.43 signal and it is assigned C-1′.

The downfield signals (8.14, 126.46) ppm indicates that the two aromatic C-H are at position 3′, 5′ and are neighbor to another aromatic carbon directly attached to a strong electron-withdrawing group (the most deshielded carbon on the spectrum), this was also confirmed by (8.14, 150.43) ppm correlation. The presence of a strongly electron-withdrawing group was further proven by the FTIR absorption band at 1498 $cm^{-1}$ in table 2 characteristic of nitro group ($NO_2$) asymmetric stretching. Therefore carbon-13 peak at

150.43 ppm was assigned to C-4′ for that reason. This conforms to the structure of ring B within the compound structure.

The three doublet signals on the proton NMR spectrum; 8.05 ppm integrating for one hydrogen, 7.65 ppm integrating for one hydrogen, and 7.47 ppm integrating for one proton as well were found coupled in COSY cross-peaks (8.05, 7.43) ppm and (7.66, 7.46) ppm respectively. The coupling constant for a peak at 8.05 ppm and 7.47 ppm were 8.5 Hz and 8.6 Hz suggesting that these hydrogens are ortho to each other. Moreso, the coupling constant for a peak at 7.65 ppm was 1.8 Hz which also suggests that this proton is meta coupled with another proton. These protons peaks were found to be directly attached to respective carbon-13 peaks on the HSQC spectrum as follows (7.66, 129.65) ppm, (7.47, 128.22) ppm, and (8.08, 127.93) ppm. It only makes sense to say signals at (7.66, 129.65) ppm are meta to signals at (7.47, 128.22) ppm. As such are assigned as C-H at position 3, C-H at position 5, and C-H at position 6 respectively. Moreover, carbon-13 peaks at 134.36 ppm, 133.16 ppm, 131.39 ppm are couple to no proton signals on the HSQC spectrum which indicates that they are substituted aromatic carbons.

A correlation between imine proton at 8.27 ppm and carbon-13 peak at 131.19 ppm was observed on HMBC spectrum, also imine proton at 8.27 ppm and carbon-13 peak at 127.74 ppm for C-6 was observed, proton 6 at 8.04 ppm and imine carbon-13 peak at 136.30 ppm on HMBC spectrum all indicated a direct linkage between the imine group and ring A. It can be deduced that the hydrazone functional group is the bridge linking the two benzene rings. Hence carbon-13 peak at 131.19 ppm was assigned C-1. The FTIR absorption signal at 1043 $cm^{-1}$ has been characterized for aromatic C-Cl stretching. Therefore the downfield carbon-13 peaks at 134.34 ppm and 133.16 ppm are directly attached to chloro groups. A careful examination of the compound structure revealed that C-2 is more deshielded due to the cumulative inductive effect from imine group nitrogen and C-4 chlorine which are each three bonds away compared to C-4 which is only weakly deshielded by C-2 chlorine. Therefore, carbon-13 peak at 134.34 ppm is assigned to C-2 while carbon-13 peak at 133.16 ppm is assigned to C-4 respectively. Accordingly, this agrees with the compound's ring A of compound 3a.

3.3.2. Structure elucidation of compound 3b (bright yellow powder).

**(*E*)-1-(3,5-dichlorobenzylidene)-2-(4-nitrophenyl)hydrazine**

For compounds (E)-1-(3,5-dichlorobenzylidene)-2-(4-nitrophenyl) hydrazine (3b). The FTIR absorption signals at 3254 $cm^{-1}$, 3075 $cm^{-1}$, and 1580 $cm^{-1}$ suggested the stretchings of secondary N-H bond, C-H bond, and C=N bond respectively in table 2. The emergence of these bonds was confirmed by the non-occurrence of carbonyl proton and carbon diagnostic peaks and appearance of singlet proton peaks at 11.55 ppm, 7.98 ppm, with carbon-13 peak at 139.44 ppm on 1H and 13C NMR spectra respectively in table 4. The proton peak at 7.94 ppm was found to couple with the carbon-13 peak at 138.66 ppm on the HSQC spectrum confirming the formation of azomethine C-H bond. More so, the two protons were coupled at (11.47, 7.87) ppm on the COSY spectrum indicating that they are neighboring protons to each other. This further substantiates the formation of the hydrazone functional group. Also, the proton at peak 11.18 ppm was observed to couple to no carbon on HSQC, this implies that it is bonded to a heteroatom which is consistent with FTIR absorption signal for N-H bond. These indicated the formation of a new hydrazone bond. Finally, HMBC correlation between N-H proton and azomethine carbon at (11.51, 138.84) ppm was noticed on HMBC spectrum affirming the synthesis of hydrazone functional group.

Absorption signals at 1416 $cm^{-1}$ and 1271 $cm^{-1}$ in tale 2 correspond to aromatic C=C stretching and C-H in-plane bending which suggests the presence of aromatic ring(s) in the compound. The presence of doublet and singlet proton peaks within the aromatic chemical shift on the proton spectrum. The carbon-13 spectrum indicated nine peaks within the aromatic chemical shift which indicates that there is more than one aromatic

ring in the structure of the compound. HSQC spectrum showed coupling between peaks at (8.12, 126.35) ppm, (7.53, 128.25) ppm, (7.73, 124.83) ppm, and (7.21, 112.11) ppm which indicates aromatic C-H bonds present in the compound. Additionally, the doublet proton peaks at 8.15 ppm and 7.25 ppm are each integrating for two hydrogens. This suggests that their respective carbon-13 peaks at 126.35 ppm and 112.11 ppm are each resonating for two equivalent carbons as well. The two proton peaks were noticed to couple at (8.14, 7.18) ppm on the COSY spectrum which indicates that they are neighboring protons to each other, the coupling constant of the two protons peaks are 9.1 Hz and 8.1 Hz respectively suggesting that each of the peaks is resonating for two protons that are ortho to each other.

The HMBC correlation at (11.53, 113.00) ppm involving N-H proton suggested that the four aromatic C-H at (8.12, 126.35) ppm and (7.21, 112.11) ppm are on ring B (hydrazine ring). Carbon-13 peaks at 150.46 ppm and 142.24 ppm were noticed to couple to no hydrogen on the HSQC spectrum indicating that they are substituted aromatic carbons. Also, the HMBC correlation at (8.12, 150.46) ppm indicates that the carbon-13 peak at 150.46 ppm is also on ring B. Furthermore, absorption signals at 1476 $cm^{-1}$ and 1297 $cm^{-1}$ corresponded to $NO_2$ asymmetric stretching and amino C-N stretching respectively in table 2. Hence, the carbon-13 peak at 150.46 ppm is assigned to position 4′ of the ring while 142.24 ppm is assigned to position 1′ of the ring as well as indicated in table 4. Similarly, the downfield coupled peaks at (8.12, 126.35) ppm on the HSQC spectrum in figure 4.27 are assigned to the equivalent C-H at positions 3′ and 5′ of the ring. The upfield coupled peaks at (7.21, 112.11) ppm are assigned to the equivalent C-H at positions 2′ and 6′ of the ring as revealed in table 4. These analyses conform to the structure of ring B and hence its presence is confirmed.

On the other hand, the HMBC spectrum in figure 4.28 revealed the correlation of imine carbon at 138.79 ppm to proton peak at 7.79 ppm which suggests that the protons responsible for the signal are on ring A. The two singlet proton peaks were coupled to their respective carbons as follows (7.53, 128.25) ppm, (7.73, 124.83) ppm on the HSQC spectrum in figure 4.27. The singlet proton peak at 7.79 ppm was found to integrate for two hydrogens suggesting that each of the equivalent aromatic hydrogens is coupled to equivalent aromatic carbons. As such, the two equivalent C-H are assigned to positions 2 and 6 of ring A. Also, C-H at (7.53, 128.25) ppm is assigned to position 4 of ring A. These assignments were further confirmed by the meta coupling of the two proton peaks at (7.69, 7.50) on the COSY spectrum in figure 4.25. Their meta coupling was also confirmed by the HMBC correlations between their protons and carbons at (7.55, 124.86) for H-4 and C-2,6 and (7.76, 128.38) ppm for H-2,6 and C-4 respectively as indicated in table 4.

The position 2 and 6 protons were correlated to another carbon at (7.79, 134.70) ppm. This carbon at 134.70 ppm was noticed to be substituted aromatic carbon on the HSQC spectrum as it does not couple with any proton. Therefore, it is assigned to carbon at position 1. Also, the downfield carbon-13 peak at 139.44 ppm was observed coupled to no proton on the HSQC spectrum which suggests that it is a substituted aromatic carbon as well. FTIR absorption signal at 957 cm-1 corresponds to aromatic C-Cl stretching confirming the presence of chloro groups on substituted carbons at 139.44 ppm which is more deshielded compared to C-1 at 134.70 ppm. Also, the carbon-13 peak at 139.44 ppm has equal intensity to those of C-2,6 and C-2′,6′ which indicates that it is resonating for two carbons as those of the latter. Thus, 13C peak at 139.44 ppm is assigned to carbon 3 and 5 of ring A. These analyses are consistent with the structure of compound 3b. Therefore, its synthesis is confirmed successfully.

3.3.3. Structure elucidation of compound 3c (brick red powder).

**(E)-1-(4-nitrophenyl)-2-(3,4,5-trimethoxybenzylidene)hydrazine**

The FTIR absorption signals at 1591 $cm^{-1}$ and 2929 $cm^{-1}$ corresponding to imine C-H and C=N bond stretchings respectively in table 2 suggest the formation of a new

azomethine bond. The absence of aldehyde characteristic proton chemical shift and carbon characteristic chemical shift on $^{1}$H-NMR and $^{13}$C-NMR spectra respectively and the appearance of a singlet proton peak at 7.97 ppm integrating for one hydrogen and C-13 peak at 142.24 ppm in table 5 authenticated the presence of C=N and imine C-H bond thus indicated the formation of new imine bond. The direct attachment of imine proton to imine carbon was observed at (7.97, 141.66) ppm on the HSQC spectrum, thus confirming the formation of the imine bond.

Furthermore, the imine proton at 7.97 ppm was found coupled to another singlet proton peak at 11.30 ppm on the COSY spectrum which integrated for one hydrogen on the proton spectrum. This suggests that the two protons are neighbors to each other. More so, a secondary amino group (N-H) bond stretching was noticed at 3283 $cm^{-1}$ in the FTIR spectrum as indicated in table 5. Considering that the proton peak at 11.30 ppm was not coupled to any carbon on the HSQC spectrum also indicated that it is attached to a heteroatom which may be nitrogen, therefore, suggesting a hydrazone functional group. Again, the nitrogen proton (N-H) peak at 11.30 ppm was correlated to the imine carbon peak at 141.91 ppm on the HMBC spectrum in table 5 and as such confirmed the synthesis of a hydrazone.

Compared to the compound 3c structure it was noticed that there were only eleven carbon-13 chemical shifts on the C-13 MNR spectrum pointing out the presence of equivalent carbons signal on the spectrum. The presence of aromatic rings was also confirmed by the FTIR absorption signals at 1412 cm-1 and 1379 cm-1 corresponding to aromatic C=C and C-H stretching and in-plane bending. On the proton NMR spectrum, there is one singlet peak at 7.05 ppm resonating for two hydrogens and two doublet peaks at 8.13 ppm and 7.19 ppm each also resonating for two hydrogens all within aromatic proton chemical shift. Coupling constants for the doublets peaks are 8.7 Hz and 7.6 Hz respectively implying that each of the two hydrogens is ortho coupled.

The doublets peaks are noticed to couple to each other as shown in the COSY spectrum (8.16, 7.18) ppm which indicates that they are next to each other on the same benzene ring. Also, these doublet protons were observed to be attached directly to their respective carbons on the HSQC spectrum (8.13, 126.02) ppm and (7.19, 111.24) ppm. These revealed that the peaks at 126.02 ppm and 111.24 ppm on the C-13 NMR spectrum are each integrating for two carbons. The gap in their chemical shift can only be accounted for by their chemical environment which suggests that carbons at 126.02 ppm are closer to an electron-withdrawing group than carbons at 111.24 ppm. Harmonizing the multiplicity, integration of these protons and carbon chemical shifts, and subsequent review of the two benzene rings of compound TMB345, only ring B (hydrazine ring) has substituted electron-withdrawing and electron-donating groups. FTIR absorption signal at 1125 $cm^{-1}$ corresponds with C-N stretching. In addition, the absorption signal at 1494 $cm^{-1}$ frequency corresponding to nitro group ($NO_2$) asymmetric stretching was also noticed on the FTIR spectrum as revealed in table 5.

Furthermore, HMBC correlation of protons and carbon peaks (8.13, 138.27) ppm and correlation of protons with carbon at (7.20, 138.27) ppm were observed. More so, the carbon peak at 138.27 ppm was not coupled to any proton on HSQC which suggests that it is a substituted aromatic carbon. Thus, it only makes sense to assign (8.13, 126.02) ppm to C-H at positions 3′ and 5′ which are next to peak C-4′ that is substituted with the nitro group. In the same vein, (7.19, 111.24) ppm may be assigned to C-H at positions 2′ and 6′ of the ring. The amino proton (N-H) and protons 3′ and 5′ were correlated with carbon-13 peak at 150.65 ppm as observed on HMBC spectrum (11.30, 150.65) ppm and (8.13, 150.65) ppm respectively. It was also noticed that the carbon peak at 150.65 ppm was not coupled with any proton on HSQC implying that it is a substituted aromatic carbon. Critical analysis of these correlations shows that the two proton signals can only correlate to C-1′. Again, N-H proton was correlated with equivalent carbons at positions 2′,6′ as indicated on the HMCB spectrum (11.30, 111.33) ppm. As such, ring B is elucidated and numbered accordingly as shown in table 5.

The observed correlations involving imine proton including (7.96, 130.05) ppm, (8.00, 103.75) on the HMBC spectrum suggested one of the two carbons is directly linked to the hydrazone bridge through the imine group. Another correlation was observed between a singlet proton peak resonating for two hydrogens at 7.06 ppm and a carbon-13 peak at 130.05 ppm. It was also noticed that the aromatic proton was coupled to carbon-13 peak at 103.75 ppm on HSQC spectrum which suggests that the carbon-13 chemical shift at 103.57 ppm is resonating for two equivalent carbons.

In addition, carbon-13 peak at 130.05 ppm was found to couple with no hydrogen implying that it is a substituted aromatic carbon. Cross analysis revealed that the substituted carbon at 130.05 ppm is directly attached to the imine group and carbon-13 peak at 103.75 and thus assigned C-1 of ring A. The equivalent aromatic C-H signals (7.06, 103.75) ppm was assigned to C-H at positions 2 and 6 of ring A. Furthermore, carbon-13 peaks at 153.60 ppm and 139.02 ppm were noticed not to couple with no hydrogen on the HSQC spectrum as indicated indicating that they are also substituted aromatic carbons. HMBC correlations (7.06, 153.60) ppm, (7.04, 138.65) ppm suggest that each of the carbons is at least two bonds away from protons at positions 2 and 6 of the benzene ring.

Absorption signals for methoxy C-H and C-O-C stretchings at frequencies 2840 $cm^{-1}$ and 1289 $cm^{-1}$ were noticed on the FTIR spectrum tabulated in table 2. These are in line with observed methyl protons resonating upfield at peaks 3.85 ppm and 3.69 ppm integrating for six and three protons respectively. These protons do not cross peak with other protons on the COSY spectrum which indicates that they are stand-alone substituted methyl protons. Moreover, the protons were found directly attached to carbon-13 upfield peaks at 55.76 ppm and 59.91 ppm respectively on the HSQC spectrum suggests that they are methoxy carbons.

Furthermore, on the HMBC spectrum correlation of the methoxy protons and carbon-13 peaks were found as follows (3.67, 55.98) ppm and (3.88, 60.12) ppm respectively indicating that the methoxy groups are next to each other. The proton peak at 3.85 ppm integrating for six hydrogens indicated that there are two methoxy groups in the same environment. Also, HMBC correlation between the methoxy protons and benzene carbons were observed at (3.73, 138.67) ppm, (3.84, 153.28) ppm suggests the direct linkage between the methoxy groups to the respective carbons. Again these also revealed that (3.84, 153.28) ppm is for two methoxy groups on two equivalent carbons and as such assigned to C-3 and C-5 of ring A. Thus, (3.73, 138.67) ppm is assigned to C-4 of ring A. These analyses were found to conform to the ring A structure. Consequently, the compound structure is elucidated. The success of the synthesis is thus confirmed.

3.3.4. Structure elucidation of compound 3d (Dark brown powder).

**(*E*)-1-(4-methoxybenzylidene)-2-(4-nitrophenyl)hydrazine**

The absorption signal at 3261 $cm^{-1}$, 3000 $cm^{-1}$, and 1595 $cm^{-1}$ on FTIR spectrum corresponds to N-H, imine C-H, and C=N stretchings respectively in table 2. The presence of these functionals was confirmed by the absence of carbonyl proton and carbon-13 diagnostic peaks on proton and carbon-13 NMR spectra and the emergence of singlet proton peaks at 11.18 ppm and 7.99 ppm integrating for one hydrogen each and carbon-13 peak at 142.41 ppm on $^{1}H$ and $^{13}C$ NMR spectra respectively in table 6 suggests the formation of a new bond. The two proton peaks were found to couple (11.18, 7.96) ppm on the COSY spectrum which indicates that they are next to each other. This is a strong indication of new hydrazone bond formation.

More so, proton peak at 8.00 ppm was noticed to couple with carbon-13 peak at 142.09 ppm on HSQC spectrum indicating that they are directly bonded to each other. This confirmed the presence of the imine C-H bond. Meanwhile, the proton at peak 11.18 ppm was observed to couple to no carbon on the HSQC spectrum, this implies that it is bonded to a heteroatom which is in line with the FTIR absorption signal for the N-H bond in table 2. These indicated the formation of a new hydrazone bond. Furthermore, HMBC correlation

between N-H proton and imine carbon was observed at (11.22, 142.03) ppm on the HMBC spectrum which authenticated the synthesis of the hydrazone functional group.

FTIR absorption signals at 1468 $cm^{-1}$ and 1271 $cm^{-1}$ corresponding to aromatic C=C stretching and C-H in-plane bending suggested the presence of aromatic rings. This was strengthened by the presence of multiple doublet peaks within the aromatic chemical shifts. These indicated the possible presence of more than one benzene ring in the structure. The four doublet proton peaks at 8.11 ppm, 7.66 ppm, 7.12 ppm, and 6.99 ppm are each integrating for two hydrogens with coupling constants 8.8 Hz, 8.2 Hz, 7.0 Hz, and 8.2 Hz respectively on the $^{1}H$ NMR spectrum. Integration of eight aromatic hydrogens is an indication of at least two benzene rings. More so, their coupling constants interpret that those on the same ring are ortho to each other. COSY spectrum for compound 3d revealed the following couplings: (8.08, 7.15) ppm and (7.66, 6.96) ppm which implies that the two hydrogens responsible for doublet peak at 8.11 ppm are ortho to the two hydrogens responsible for doublet peak at 7.12 ppm, therefore are on the same ring. Likewise, the two hydrogens responsible for the doublet peak at 7.66 ppm and the two hydrogens responsible for the doublet peak at 6.99 ppm are also on the same ring and are ortho to each other. These analyses conform to the structure of 3d.

Furthermore, the presence of nine peaks within the aromatic chemical shift on the $^{13}C$ NMR spectrum further, buttresses these claims. It was discovered that the four doublet proton peaks were coupled to their respective carbons (8.11, 126.32) ppm, (7.68, 128.15) ppm, (7.14, 111.08) ppm, and (7.01, 114.40) ppm on the HSQC spectrum. Considering that each of the doublet protons peaks is integrating for two aromatic hydrogens indicated that each of these carbon-13 peaks they coupled to on HSQC spectrum is also resonating for two equivalent aromatic carbons. Hence, the two equivalent aromatic carbons responsible for carbon-13 peak at 126.32 ppm are ortho to the two equivalent aromatic carbons responsible for a peak at 111.08 ppm on the same ring. Similarly, carbon-13 peaks at 128.15 ppm and 114.40 ppm are each resonating for two equivalent aromatic carbons and are ortho to each other on the same ring. These analyses also confirm the presence of two benzene rings in the compound 3d structure.

HMBC spectrum revealed the correlation (11.17, 111.08) ppm between the amino proton and carbon-13 peak at 111.08 ppm suggest that these carbons are on ring B (hydrazine ring). The correlations viz; (7.14, 138.14) ppm, (8.13, 138.13) ppm, and (8.13, 150.97) ppm also suggest that these protons and carbons are on ring B. More so, carbon-13 peaks at 138.14 ppm and 150.97 ppm were noticed to couple with no hydrogen on the HSQC spectrum which indicates that they are substituted aromatic carbons. Additionally, their downfield chemical shifts suggested they are directly bonded to electronegative atoms. The FTIR absorption signal at 1168 $cm^{-1}$ in table 2 corresponds to the C-N stretching of amine. This indicates the presence of a strongly electron-donating group and the resultant upfield chemical shift of its neighboring protons and carbons. As such carbon-13 peak at 138.14 ppm is assigned to C-1′ in table 6. Consequently, upfield peaks at (7.14, 111.08) ppm are assigned to positions 2′ and 6′ of ring B in table 6. Further analysis also suggests that carbon at 150.97 ppm is bonded to an electron-withdrawing group. The absorption signal at 1509 $cm^{-1}$ corresponds to $NO_2$ group asymmetric stretching in table 2 confirming the substitution of $NO_2$ on carbon at 150.97 ppm chemical shift. Therefore, this carbon is assigned C-4′ as indicated in table 6. It was observed that the downfield peaks at (8.11, 126. 32) ppm are due to the inductive effect from the $NO_2$ group at C-4′ and are therefore assigned to positions 3′ and 5′of the ring B as indicated in table 6. These analyses are consistent with the structure of ring B.

The observed correlations involving imine proton and carbon as follows; (8.11, 126.83) ppm and (7.64, 142.28) ppm suggest C-H coupling on HSQC at (7.68, 128.15) ppm and C-H at (7.01, 114.40) ppm are on ring A and are linked to ring B by hydrazone bridge. More so, carbon-13 peaks at 160.55 ppm and 127.49 ppm were noticed to couple with no hydrogen which indicates that they are substituted aromatic carbons. The FTIR absorption signal at 2832 $cm^{-1}$ and 1241 $cm^{-1}$ suggests the methoxy C-H stretching and C-O-C

stretching respectively in table 2. The upfield singlet proton peak at 3.79 ppm integrating for three hydrogens on the $^{1}$H-NMR spectrum was noticed to couple with carbon-13 peak at 55.26 ppm on HSQC spectrum which suggests the presence of methyl group. Furthermore, the methyl proton peak was observed to correlate only with the downfield carbon-13 peak at 160.53 ppm on the HMBC spectrum confirming the presence of the methoxy group. Therefore, the carbon-13 peak at 160.53 ppm is assigned C-4 while the carbon-13 peak at 126.83 ppm is assigned C-1 in table 6. HMBC correlation between doublet proton peak at 7.65 ppm and imine carbon peak at 142.28 ppm confirms the position of (7.68, 128.15) ppm signal and are assigned to C-H at position 2 and 6 of ring A in table 6. Consequently, (7.01, 114.40) ppm signals are assigned to C-H at positions 3 and 5 on ring A in table 6. These analyses are consistent with the compound 3d structure and thus the synthesis of compound 3d was confirmed successfully.

The $^{1}$H and $^{13}$C NMR spectra chemical shifts of 3d were found to agree with the $^{1}$H and $^{13}$C NMR spectra chemical shifts reported by Shikhaliyev *et al*. [35] for the same compound.

## 4. Materials and Methods

All the reagents used were purchased from Sigma Aldrich, and they were used with no further purification. Electrothermal Engineering LTD 9100 apparatus was employed in the melting points determination of the synthesized compounds. The FTIR spectra were recorded on Agilent technologies spectrometer model 543, and the 1H and 13C NMR spectra were obtained using a Brucker AMX 400 MHz spectrometer operating at 400 MHz and 101 MHz respectively with dimethyl sulfoxide (DMSO) used as the solvent. Chemical shifts (δ) are reported in parts per million and are referenced to the NMR solvent peak.

General procedure: Synthesis of p-nitrophenyl hydrazones 3a-b

### *4.1. Solvent-based procedure*

5.09mmol of each of the benzaldehydes 1a-d and p-nitrophenyl hydrazine 2 were dissolved in 30 ml of ethanol. This was followed by the addition of five drops of glacial acetic acid as a catalyst. The mixture was magnetically stirred for three hours. The reactions were carried out at room conditions. The progress of the reaction was monitored by TLC. Upon completion, the crude products were filtered, dried then transferred into a beaker.

### *4.2. Solvent-free procedure*

Equimolar quantities of p-nitrophenyl hydrazine 2 (1 mmol; ) and each of the aromatic aldehydes 1a-d (1 mmol) were grounded in a universal tube with the aid of a glass rod for 5 minutes. The reactions were carried out at room conditions. The progress of the reaction was monitored by TLC. On completion, the mixture product was transferred into a beaker.

### *4.3. Purification (work-up)*

20 ml of cold 2 M hydrochloric acid was added and stirred to scavenge the possible unreacted p-nitrophenyl hydrazine 2. The product precipitate was filtered off, dried, and subsequently washed with 30 ml of cold distilled water and 20 ml of cold 95% ethanol step-wisely to afford colored powdered products 3a-d in high to excellent yield.

## 5. Conclusions

Summarily, we have successfully synthesized novel dichloro and trimethoxy p-nitrophenyl hydrazones using a solvent-free method and the modified existing solvent-based method of condensation. Easy and efficient workups, unsolvated pure products in high to excellent yields are the advantages of this modified method. At the end of this experiment, all the compounds were obtained at high to excellent yield using the solvent-

based method which was superior to solvent-free yields. The generality and simplicity of the technique, catalyst-free conditions, non-use of an organic solvent, the short reaction time, and the easy and efficient workup, unsolvated pure products in moderate to high yields are all the advantages of the developed solvent-free method.

**Author Contributions:** Conceptualization, Babalola Sodeeq A.; Idris Abdullah and Hamza Asmau; methodology, Babalola Sodeeq A.; software, Babalola Sodeeq and Hamza Asmau; validation, Idris Abdullah Y. and Sanni Y. M.; formal analysis, Babalola Sodeeq A.; investigation, Babalola Sodeeq A; resources, Hamza Asmau, Muhammad Hayatudeen Y., Erumiseli Oshoma; data curation, Lateef Bakare; writing—original draft preparation, Babalola Sodeeq A.; writing—review and editing, Igie Nosakhare; visualization, Babalola Sodeeq A.; supervision, Idris Abdullah Y. and Sanni Y. M.;

All authors have read and agreed to the published version of the manuscript.

**Funding:** This research received no external funding.

**Data Availability Statement:** Not applicable.

**Acknowledgments:** We acknowledge Dr. Olayiwola Bello of the University of Ilorin for moral and financial support.

**Abbreviation**

COSY: Correlation spectroscopy

HSQC: Heteronuclear single quantum coherence

HMBC: Heteronuclear multiple bond coherence

**Conflicts of Interest:** The authors declare no conflict of interest. The funders had no role in the design of the study; in the collection, analyses, or interpretation of data; in the writing of the manuscript, or in the decision to publish the results.

**Supplementary Materials:** The following supporting information can be downloaded at: www.mdpi.com/xxx/s1, Figure S1: title; Table S1: title; Video S1: title.

## References

1. Singh A.K., Thakur S., Pani B., B. Chugh B., Lgaz H. *et al*. Solvent-free microwave-assisted synthesis and corrosion inhibition study of a series of hydrazones derived from thiophene derivatives: Experimental, surface, and theoretical study. J. Mol. lipids (2019). https://doi.org/10.1016/j.molliq.2019.03.126
2. Sainath Zangade and Pravinkumar Patil. A Review on Solvent-free Methods in Organic Synthesis. Current Organic Chemistry, 23, (2019) 2295-2318.
3. Hossein Naeimi, Hashem Sharghi, Fariba Salimi, and Khadijeh Rabiei. Facile and Efficient Method for Preparation of Schiff Bases Catalyzed By P2O5/SiO2 under Free Solvent Conditions. Heteroatom Chemistry Volume 19, Number 1 (2008).
4. V. Koteswara Rao, S. Subba Reddy, B. Satheesh Krishna, K. Reddi Mohan Naidu, and C. Naga Raju. Synthesis of Schiff's bases in aqueous medium: a green alternative approach with effective mass yield and high reaction rates. Green Chemistry Letters and Reviews Vol. 3, No. 3, September 2010, 217-223. Taylor & Francis.
5. Duha Adnan, Bijender Singh, Surinder Kumar Mehta, Vinod Kumar, and Ramesh Kataria. Simple and solvent-free practical procedure for chalcones: An expeditious, mild and greener approach. Current Research in Green and Sustainable Chemistry 3, (2020) 100041.
6. Sunita Bhagat, Nutan Sharma, and Tejpal Singh Chundawat. Synthesis of Some Salicylaldehyde-Based Schiff Bases in Aqueous Media. Journal of Chemistry, Volume2013, Article ID 909217, (2013) 4 pages. http://dx.doi.org/10.1155/2013/909217. Hindawi Publishing Corporation.
7. Abbas Shockravi, Mahdieh Sadeghpour, and Abolfazl Olyaei. Simple and Efficient Procedure for the Synthesis of Symmetrical Bis-Schiff Bases of 5,5′-Methylenebis(2-aminothiazole) Under Solvent-free Conditions. Synthetic Communications 1, (40) (2010). 2531–2538. Taylor & Francis Group, LLC.
8. Mehtab Parveen, Shaista Azaz, Ali Mohammed Malla, Faheem Ahmad, and Pedro Sidonio Pereira da Silva *et al*. Solvent-free, [Et3NH][HSO4] catalyzed facile synthesis of hydrazone derivatives. RSC (2014). DOI: 10.1039/c4nj01666a
9. Pierrick Nun, Charlotte Martin, Jean Martinez, Frédéric Lamaty. Solvent-free synthesis of hydrazones and their subsequent N-alkylation in a Ball-mill. Tetrahedron, Elsevier, 67 (42), (2011) pp. 8187-8194. 10.1016/j.tet.2011.07.056. hal-00623809
10. Mo Zhang, Ze-Ren Shang, Xiao-Tang Li, Jia-Nan Zhang, Yong Wang *et al*. An International Journal for Rapid Communication of Synthetic Organic Chemistry Volume 47, (2017). https://doi.org/10.1080/00397911.2016.1258476

11. Noor ul Ain, Tariq Mahmood Ansari, M. Rehan H. Shah Gilani, Guobao Xu, Gaolin Liang. Facile and straightforward synthesis of Hydrazone derivatives. Hindawi Journal of Nanomaterials. Volume (2022), Article ID 3945810, 6 pages https://doi.org/10.1155/2022/3945810
12. Jana Pisk, Ivica Đilovic, Tomica Hrenar, Danijela Cvijanovic, Gordana Pavlovic *et al*. Effective methods for the synthesis of hydrazones, quinazolines, and Schiff bases: reaction monitoring using a chemometric approach. RSC Adv., (2020), 10, 38566
13. Pierrick Nun, Charlotte Martin, Jean Martinez, Frédéric Lamaty. Solvent-free synthesis of hydrazones and their subsequent N-alkylation in a Ball-mill. Tetrahedron, Elsevier, 67 (42), (2011) pp. 8187-8194. 10.1016/j.tet.2011.07.056. hal-00623809
14. Mehtab Parveen, Shaista Azaz, Ali Mohammed Malla, Faheem Ahmad, Pedro Sidonio Pereira da Silva et al. Solvent-free, [Et3NH][HSO4] catalyzed facile synthesis of hydrazone derivatives. Royal Society of Chemistry (2014). DOI: 10.1039/c4nj01666a
15. Oliveira P. F. M., Baron M., Chamayou A., Andre-Barr`es C., Guidettib B. and Baltas M. Solvent-free mechanochemical route for green synthesis of pharmaceutically attractive phenol hydrazones. RSC Advances, Royal Society of Chemistry, 2014, 4 (100), p.56736-56742. 10.1039/c4ra10489g. hal-01625025
16. Harith M. Al-Ajely and Aymen N. Yassen. Microwave Synthesis of some Substituted Hydrazones under Solvent-Free Conditions. International Journal of Scientific & Engineering Research Volume 8, Issue 5, May-2017 1854 ISSN 2229-5518
17. Singh A.K., Thakur S., Pani B., B. Chugh B., Lgaz H. et al. Solvent-free microwave-assisted synthesis and corrosion inhibition study of a series of hydrazones derived from thiophene derivatives: Experimental, surface, and theoretical study. Journal of Molecular lipids (2019). https://doi.org/10.1016/j.molliq.2019.03.126
18. Crawford, D. E., Porcheddu, A., McCalmont, A. S., Delogu, F., James, S. L. et al. Solvent-free, Continuous Synthesis of Hydrazone-Based Active Pharmaceutical Ingredients by Twin-Screw Extrusion. ACS Sustainable Chemistry & Engineering, 8(32), (2020) 12230-12238.https://doi.org/10.1021/acssuschemeng.0c03816
19. Hayder M. Abdulhamza and Muthanna S. Farhan. Synthesis, Characterization and Preliminary Anti-inflammatory Evaluation of New Fenoprofen Hydrazone Derivatives. Iraqi J Pharm Sci, Vol. 29 (2) (2020).
20. Wang Shi-Meng, Gao-Feng Zha, K. P. Rakesh et al. Synthesis of benzo[d]thiazole-hydrazone analogs: molecular docking and SAR studies of potential H+/K+ ATPase inhibitors and anti-inflammatory agents. MedChem Comm. Royal Society of Chemistry (2017).
21. A.L.V. Kumar Reddy and Niren E Kathale. Synthesis and Anti-inflammatory Activity of Hydrazide-Hydrazones Bearing Anacardic Acid and 1,2,3-Triazole Ring Based Hybrids. Orient. J. Chem., Vol. 33(6), (2017) 2930-29 36.
22. Abadi, A.H.; Eissa, A.A.H.; Hassan, G.S. Synthesis of novel 1,3,4-trisubstituted pyrazole derivatives and their evaluation as antitumor and antiangiogenic agents. Chem. Pharm. Bull. 51, (2003) 838-844.
23. Ziad Moussa, Mohammed Al-Mamary, Sultan Al-Juhani et al. Preparation and biological assessment of some aromatic hydrazones derived from hydrazides of phenolic acids and aromatic aldehydes. Heliyon 6; (2020). e05019. www.cell.com/heliyon.
24. Lee Y. J., Jeong W. K., Shin S., Lee U. J. and Kim Y. Discovery of novel selective inhibitors of Staphylococcus aureus β- ketoacyl acyl carrier protein synthase III, Eur. J. Med. Chem., 47, (2012) 261-269.
25. El-Sabbagh OI., Shabaan MA., Kadry HH. And Al-Din ES. New octahydroquinazoline derivatives: Synthesis and hypotensive activity, Eur. J. Med. Chem., 45, (2010) 5390-5396.
26. Ragavendran, J.; Sriram, D.; Patel, S.; Reddy, I. and Bharathwajan, N. et al. Design and synthesis of anticonvulsants from a combined phthalimide-GABA-anilide and hydrazone pharmacophore. Eur. J. Med. Chem. 42, (2007) 146-151.
27. Ergenç, N.; Günay, N.S. Synthesis and antidepressant evaluation of new 3-phenyl-5-sulfonamidoindole derivatives, Eur. J. Med. Chem. 1998, 33, 143-148.
28. Nawaf A. Alsaif, Mashooq A. Bhat, Mohamed A. Al-Omar, Hanaa M. Al-Tuwajiri, Ahmed M. Naglah et al. Synthesis of Novel Diclofenac Hydrazones: Molecular Docking, Anti-Inflammatory, Analgesic, and Ulcerogenic Activity. Journal of Chemistry (2020). Hindawi https://doi.org/10.1155/2020/4916726
29. Abdel-Aal, M.T.; El-Sayed, W.A.; El-Ashry, E.H. Synthesis and antiviral evaluation of some sugar arylglycinoylhydrazones and their oxadiazoline derivatives. Arch. Pharm. Chem. Life Sci. (2006), 339, 656-663.
30. Bukowski L.; Janowiec, M. 1-Methyl-1H-2-imidazo[4,5-b]pyridinecarboxylic acid and some derivatives with suspected antituberculotic activity. Pharmazie, 51, (1996) 27-30.
31. Gemma, S.; Kukreja, G.; Fattorusso, C.; Persico, M.; Romano, M.; Altarelli, M.; Savini, L.; Campiani, G.; Fattorusso, E.; Basilico, N. Synthesis of N1-arylidene-N2-quinolyl- and N2-acrydinylhydrazones as potent antimalarial agents active against CQ-resistant P. falciparum strains. Bioorg. Med. Chem. Lett. (2006), 16, 5384-5388.
32. Jordao A. K., Sathler PC., Ferreira VF., Campos VR., de Souza MCBV. et al. Synthesis, antitubercular activity, and SAR study of N-substituted phenylamino-5-methyl-1H-1,2,3-triazole-4-carbohydrazides, Bioorg. Med. Chem., 19, (2011), 5605-5611.
33. Silva, A.G.; Zapata-Suto, G.; Kummerle, A.E.; Fraga, C.A.M.; Barreiro, E.J. et al. Synthesis and vasodilatory activity of new N-acyl hydrazone derivatives, designed as LASSBio-294 analogs. Bioorg. Med. Chem. 13, (2005) 3431-3437.
34. Gage JL., Onrust R., Johnston D., Osnowski A., MacDonald W. N-Acylhydrazones as inhibitors of PDE10A, Bioorg. Med. Chem. Lett., 21, (2011) 4155-4159.
35. Shikhaliyeva N. G., Askerovaa U. F., Mukhtarovaa S. H., Niyazovaa A. A. (2019). Synthesis and Structural Study of Dichlorodiazadienes Derived from 4-Methoxybenzaldehyde. Russian Journal of Organic Chemistry, Vol. 56, No. 2, pp. 185–192. 10.1134/S1070428020020013